University Library

A gateway to Melbourne's research publications

Minerva Access is the Institutional Repository of The University of Melbourne

Author/s:
McCluskey, AH;Grant, SB;Stewardson, MJ

Title:
Flipping the thin film model: Mass transfer by hyporheic exchange in gaining and losing streams

Date:
2016-10-01

Citation:
McCluskey, A. H., Grant, S. B. & Stewardson, M. J. (2016). Flipping the thin film model: Mass transfer by hyporheic exchange in gaining and losing streams. Water Resources Research, 52 (10), pp.7806-7818. https://doi.org/10.1002/2016WR018972.

Persistent Link:
https://hdl.handle.net/11343/291802

Flipping the Thin Film Model: mass transfer by hyporheic exchange in gaining and losing streams

Alexander H. McCluskey[1] Stanley B. Grant[2] Michael J. Stewardson[1]

Accepted Article

Corresponding author: S. B. Grant, Henry Samueli School of Engineering, University of California, Irvine, USA. (sbgrant@uci.edu)

[1]Department of Infrastructure Engineering, The University of Melbourne, Australia

[2]Henry Samueli School of Engineering, University of California Irvine, California USA

D R A F T September 18, 2016, 1:42pm D R A F T
This is the author manuscript accepted for publication and has undergone full peer review but has not been through the copyediting, typesetting, pagination and proofreading process, which may lead to differences between this version and the Version record. Please cite this article as doi:10.1002/2016WR018972.

This article is protected by copyright. All rights reserved.

Abstract. The exchange of mass between a stream and its hyporheic zone, or *"hyporheic exchange"*, is central to many important ecosystem services. In this paper we show that mass transfer across the streambed by linear mechanisms of hyporheic exchange in a gaining or losing stream can be represented by a thin film model in which: (a) the mass transfer coefficient is replaced with the average Darcy flux of water downwelling into the sediment; and (b) the driving force for mass transfer is *"flipped"* from normal to the surface (concentration difference across a boundary layer) to parallel to the surface (concentration difference across downwelling and upwelling zones). Our analysis is consistent with previously published analytical, computational, and experimental studies of hyporheic exchange in the presence of stream-groundwater interactions, and links stream network, advection-dispersion, and stochastic descriptions of solute fate and transport in rivers.

Accepted Article

This article is protected by copyright. All rights reserved.

1. Introduction

Stream health and function depends on the advective exchange of nutrients and dissolved oxygen across the sediment-water interface [*Boano et al.*, 2014; *Harvey and Gooseff*, 2015], a phenomenon known as hyporheic exchange. Hyporheic exchange can be characterised by: (1) the average Darcy flux of water moving across the sediment-water interface, denoted here by the variable $\overline{u}$ [units of $m{\cdot}s^{-1}$]; and (2) the residence time distribution (RTD) of water parcels in the sediment, denoted by the function $F_{RTD}(t)$. The average Darcy flux $\overline{u}$ can be thought of as the velocity with which solutes encounter the hyporheic zone [*Boano et al.*, 2007; *Elliott and Brooks*, 1997a; *Packman et al.*, 2000]; it is zero in the limit where streamborne solutes do not undergo hyporheic exchange, as would be the case, for example, for solute transport down a concrete lined channel. On the other hand, the RTD function $F_{RTD}(t)$ represents the fraction of stream water parcels entering the hyporheic zone at time $t = 0$ that have exited by time t [*Elliott and Brooks*, 1997a, b]. Because stream water parcels take diverse paths through the hyporheic zone (some of which are short and quick, and others of which are long and slow), the F_{RTD} function for hyporheic exchange is often heavy-tailed; i.e., a large fraction of water parcels spends a relatively short time in the hyporheic zone, while a small fraction of water parcels spends a very long time in the hyporheic zone [*Haggerty et al.*, 2002; *Wörman et al.*, 2002; *Schumer et al.*, 2003; *Wörman et al.*, 2006; *Boano et al.*, 2007; *Gooseff et al.*, 2007; *Cardenas et al.*, 2008; *Marion et al.*, 2008; *Boano et al.*, 2014; *Aubeneau et al.*, 2015]. In short, the average Darcy flux is a measure of how frequently a streamborne solute encounters the hyporheic

Accepted Article

This article is protected by copyright. All rights reserved.

zone, while the RTD is a measure of how long the solute remains in the hyporheic zone before exiting.

Elucidating the physical, hydrological, and geological controls on $\overline{u}$ and F_{RTD} is an active area of current research, and much has been learned over the past twenty years from laboratory, field, and modelling studies [*Wörman et al.*, 2007; *Krause et al.*, 2011; *Boano et al.*, 2014; *Cardenas*, 2015]. Models, in particular, are useful because they provide a quantitative framework within which field and laboratory observations of hyporheic exchange can be scaled up to entire river basins [*Kiel and Cardenas*, 2014; *Gomez-Velez and Harvey*, 2014]. A number of modelling frameworks have been proposed for capturing the effects of hyporheic exchange on solute fate and transport in streams, including the transient storage model (TSM) [*Nordin and Troutman*, 1980; *Bencala and Walters*, 1983; *Runkel*, 1998]; the Variable Residence-Time (VART) model [*Deng et al.*, 2004]; Solute Transport and Multi-Rate Mass Transfer-Linear coordinates (STAMMT-L) model [*Haggerty et al.*, 2002; *Gooseff et al.*, 2007]; Fractional Advection-Dispersion Equation (FADE) [*Schumer et al.*, 2003]; Advective Storage Path (ASP) model [*Wörman et al.*, 2002]; Solute Transport in Rivers (STIR) model [*Marion et al.*, 2008]; the Continuous Time Random Walk (CTRW) model [*Aubeneau et al.*, 2015; *Boano et al.*, 2007]; the Multiscale model (MSM) [*Stonedahl et al.*, 2010, 2013]; and the Networks with Exchange and Subsurface Storage (NEXSS) model [*Gomez-Velez and Harvey*, 2014]. In general, these models can be grouped into those that: (1) couple hyporheic exchange to classic (advection-dispersion) mass balance models of solute fate and transport in rivers (TSM, VART, STAMMT-L, FADE, ASP); (2) conceptualise solute transport as a random walk in which the Darcy flux $\overline{u}$ is a measure of the *"encounter frequency"* between the solute and hyporheic zone,

Accepted Article

This article is protected by copyright. All rights reserved.

and the F_{RTD} determines how long solutes *"wait"* in the hyporheic zone before returning to the stream (STIR, CTRW); and (3) couple simple physical process-based models of groundwater-surface water interactions operating at multiple scales (MSM, NEXSS). Models in the first category differ primarily in the way solute transfer across the sediment-water interface is parameterised, and the RTDs of stream water passing through the hyporheic zone [*Cardenas*, 2015]. A fourth group of process-based models focus on the coupling of physical and biogeochemical processes associated with hyporheic exchange, including pore network models [*Briggs et al.*, 2015] and analytical or computational flow field models [*Elliott and Brooks*, 1997a; *Cardenas and Wilson*, 2007; *Boano et al.*, 2008, 2009; *Stonedahl et al.*, 2010; *Marzadri et al.*, 2011; *Kessler et al.*, 2012; *Stonedahl et al.*, 2013; *Gomez-Velez and Harvey*, 2014; *Grant et al.*, 2014; *Marzadri et al.*, 2014; *Azizian et al.*, 2015].

Regardless of which modelling approach is adopted, there remains an urgent need to better understand how hyporheic exchange and the biogeochemical transformations it fosters are affected by flow fields that operate over a wide range of temporal and spatial scales [*Boano et al.*, 2014]. For example, the upwelling of nitrate-contaminated groundwater can affect stream water quality both directly by adding nitrate, and indirectly by altering features of the hyporheic zone (redox chemistry, exchange flux, and RTD of water parcels) that influence denitrification rates [*Hester et al.*, 2013]. In this example, the interplay between small-scale (hyporheic) and regional (groundwater) flow fields controls the concentration of nitrate in the stream [*Hinkle et al.*, 2001; *Gomez-Velez et al.*, 2015].

In this paper we tackle the multi-scale nature of hyporheic exchange using a kinematic framework [*Potter et al.*, 2012] that blends elements of the various modelling approaches described above. Our analysis accommodates three-dimensional geometries and arbitrary

Accepted Article

This article is protected by copyright. All rights reserved.

hyporheic exchange flow fields provided that the equations that govern hyporheic exchange are linear. Consequently, our results should apply to a broad range of hydrogeomorphic features that drive hyporheic exchange in the field [*Hester and Gooseff*, 2010]. The paper is organised as follows. Expressions for mass flux across the sediment-water interface are derived in Section 2, followed by a discussion of RTDs in Section 3. Our results are then tested against previously published analytical, computational, and experimental studies of bedform-induced hyporheic exchange under gaining and losing conditions (Section 4) and conclusions (Section 5) are presented.

2. A Thin Film Model for Hyporheic Exchange

2.1. Overview

Hyporheic exchange involves a downstream spiralling of water and solutes between the stream and streambed [*Stream Solute Workshop*, 1990]. The flow of water and solutes into the streambed occurs in well-defined patches called downwelling zones (blue patch in the middle panel of Figure 1). Likewise, water and solutes in the interstitial pore spaces of the sediment return to the stream in well-defined patches called upwelling zones (red patch in the middle panel of Figure 1). Although flow paths through the hyporheic zone are complex and three-dimensional, it is useful to conceptualise hyporheic exchange as occurring over a defined area of the streambed, referred to here as a Representative Elemental Area (REA). The REA can be thought of as the hyporheic exchange equivalent of a representative elemental volume (REV) for flow and transport through porous media [*Bear and Cheng*, 2010]. Differently sized REAs will capture hyporheic exchange occurring at different scales: e.g., an REA on the order of a square meter might capture hyporheic exchange over ripples, whereas an REA on the order of several square kilometres might

Accepted Article

This article is protected by copyright. All rights reserved.

capture hyporheic exchange at the scale of river meanders. Thus, the choice of REA will determine the scale of hyporheic exchange under consideration.

In the next few sections we derive expressions for the net flux of mass across the sediment-water interface (J, units of $kg{\cdot}m^{-2}{\cdot}s^{-1}$) by hyporheic exchange within a REA of length λ (oriented parallel to the streamflow) and width P.

$$J = -\frac{1}{\lambda P}\left(\dot{m}_{DW} - \dot{m}_{UW}\right), \qquad \dot{m}_{DW}, \dot{m}_{UW} \geq 0 \tag{1}$$

The variables $\dot{m}_{DW}$ and $\dot{m}_{UW}$ represent mass flow rates (units of $kg{\cdot}s^{-1}$) into and out of downwelling and upwelling zones, respectively. These two quantities are calculated by integrating the product of water flux across the sediment-water interface ($\mathbf{v}_{SWI}$) and either uniform solute concentration on the stream-side of the downwelling zone (C_{DW}) or spatially-dependent solute concentration on the sediment-side of the upwelling zone (C_{UW}), respectively:

$$\dot{m}_{DW} = -C_{DW} \int_{A_{DW}} \mathbf{v}_{SWI} \cdot \hat{\mathbf{n}} dA \tag{2a}$$

$$\dot{m}_{UW} = \int_{A_{UW}} C_{UW} \mathbf{v}_{SWI} \cdot \hat{\mathbf{n}} dA \tag{2b}$$

Variables appearing here include the unit normal to the sediment-water interface ($\hat{\mathbf{n}}$, taken as positive upward), and upwelling (A_{UW}) and downwelling (A_{DW}) zone areas (blue and red patches, Figure 1). In writing equation (2a), we have assumed that the solute concentration in a stream will not vary significantly over a downwelling zone; the negative sign on the right hand side assures that $\dot{m}_{DW}$ is a positive quantity.

Accepted Article

This article is protected by copyright. All rights reserved.

Equations (1) and (2) can be combined to yield the following expression for mass flux across the sediment-water interface by hyporheic exchange with or without stream-groundwater interactions:

$$J = -k_m \left(C_{DW} - \gamma \overline{C}_{UW} \right), \qquad k_m, C_{DW}, \gamma, \overline{C}_{UW} \geq 0 \tag{3a}$$

$$\overline{C}_{UW} = \frac{\int_{A_{UW}} C_{UW} \mathbf{v}_{SWI} \cdot \hat{\mathbf{n}} dA}{\int_{A_{UW}} \mathbf{v}_{SWI} \cdot \hat{\mathbf{n}} dA} \tag{3b}$$

New variables appearing here include a mass transfer coefficient (k_m), a flow-weighted solute concentration in the upwelling zone ($\overline{C}_{UW}$), and a weighting factor (γ). The negative sign on the right hand side of equation (3a) indicates that flux is directed into the sediment ($J < 0$) whenever $C_{DW} > \gamma \overline{C}_{UW}$.

The mathematical form of equation (3a) is analogous to the thin-film model for interfacial mass flux [*Cussler*, 2009; *Grant and Marusic*, 2011] with two notable differences. Firstly, the driving force for mass transfer is the weighted concentration difference across upwelling and downwelling zones within the REA. In contrast, the driving force for mass transfer in the thin film model is the concentration difference across a boundary layer adjacent to a solid surface. By changing the direction of the driving force for mass transfer from normal to the surface (in the thin film model) to parallel to the surface (in our application), equation (3a) can be thought of as a thin film model that has been *"flipped"* on its side. Secondly, the magnitude of the mass transfer coefficient k_m in our model depends on the circulation of water between downwelling and upwelling zones within an REA. The intensity of circulation, in turn, is determined by static and dynamic pressure variations over the streambed, and stream-groundwater interactions. In contrast, the mass transfer

Accepted Article

This article is protected by copyright. All rights reserved.

coefficient in the conventional thin film model depends on turbulent and diffusive mass transport phenomena that operate at or near the solid-water interface. Thus, while the form of equation (3a) is mathematically analogous to a thin film model, both the orientation of the driving force and the underlying physics responsible for the rate of mass transfer differ substantially.

Beyond its conceptual similarity to the thin film model, equation (3a) also has a practical application: it provides a framework for incorporating the effects of rising and falling groundwater into stream network models of solute fate and transport at the watershed scale. In such models, the fraction f (unitless) of solute load removed or added over a stream reach is determined by the balance between solute transport and transformation within the streambed (as represented by the solute uptake velocity v_f, units $m{\cdot}s^{-1}$) and horizontal transport by the stream (as represented by the hydraulic loading rate H_L, units $m{\cdot}s^{-1}$) [*Wollheim et al.*, 2006]:

$$f = \left| 1 - exp\left(\frac{-v_f}{H_L}\right) \right| \tag{4}$$

This equation assumes that, over a stream reach, streamflow is steady and uniform, and solute transport is dominated by advection (i.e., longitudinal dispersion neglected). A value of $f = 0$ indicates that there is no change in solute load over the stream reach, whereas $f = 1$ indicates that 100% of the solute load is either removed (if $v_f > 0$) or added (if $v_f < 0$) over the stream reach. The hydraulic loading rate, which represents the downstream mass transport rate per unit area of the streambed, can be calculated from the stream discharge Q (units $m^3{\cdot}s^{-1}$), stream width (P), and reach length (l): $H_L = Q/lP$. The solute uptake velocity, on the other hand, is defined as the flux of solute into the

Accepted Article

This article is protected by copyright. All rights reserved.

streambed divided by the solute concentration in the stream: $v_f = -J/C_{DW}$; for the sign convention adopted here, a positive solute uptake velocity indicates net mass transfer into the sediment bed. Assuming that solute flux to the sediment bed is dominated by hyporheic exchange, v_f can be written explicitly in terms of our thin film model parameters $\overline{C}_{UW}$, k_m and γ:

$$v_f = k_m \left(1 - \gamma \frac{\overline{C}_{UW}}{C_{DW}}\right) \tag{5}$$

By expressing the solute uptake velocity in this way, two limits are immediately apparent. When all of the solute is removed by reaction within the streambed (i.e., no solute returns to the stream in upwelling zones, $\overline{C}_{UW} = 0$) the uptake velocity is said to be *"mass transfer limited"*: $v_f = k_m$. On the other hand, when the concentration of solute is unchanged by passage through the hyporheic zone ($\overline{C}_{UW} = C_{DW}$), the *"conservative solute"* limit applies: $v_f = k_m (1 - \gamma)$. Importantly, because our expressions for k_m and γ explicitly account for groundwater flux (see Sections 2.2 through 2.4), equation (5) opens up the possibility of tailoring the solute uptake velocity to reflect local and regional variability in stream-groundwater interactions and consequent affects on, for example, the fate and transport of nitrate pollution [*Gomez-Velez et al.*, 2015].

The challenge, of course, is to obtain realistic estimates for the thin film model parameters k_m, γ, and $\overline{C}_{UW}$. To this end, several approaches can be adopted. The first two parameters (k_m and γ) can be estimated from field measurements of the small-scale exchange flux, groundwater flux, and the areal extents of downwelling and upwelling zones within an REA (as outlined in Sections 2.2 through 2.4). The third parameter ($\overline{C}_{UW}$) can be estimated from the ratio of solute and water fluxes emitted from individual upwelling

Accepted Article

This article is protected by copyright. All rights reserved.

zones (see definition, equation (3b)), calculated from the residence time distribution and presumed biogeochemical reactions in the hyporheic zone (see Section 3), and/or estimated directly from equation (5) given reach-scale estimates of k_m, γ, and solute uptake velocity v_f (e.g., see *Mulholland et al.* [2008]). In the next few sections we derive expressions for k_m and γ when there is: no groundwater seepage (*"neutral stream"*) (Section 2.2); seepage of a stream into groundwater (*"losing stream"*) (Section 2.3); and seepage of groundwater into a stream (*"gaining stream"*) (Section 2.4).

The analysis presented below is premised on three key assumptions: (1) flow through the hyporheic zone is steady-state; (2) within a REA, all stream water entering a downwelling zone eventually re-emerges in an upwelling zone or is lost to groundwater; and (3) water flux at any location along the sediment-water interface ($\mathbf{v}_{SWI}$) can be expressed as the sum of water fluxes generated by hyporheic exchange in the absence of groundwater flow ($\mathbf{u}^0_{hz}$) and groundwater flow ($\mathbf{u}_{gw}$): $\mathbf{v}_{SWI} = \mathbf{u}^0_{hz} + \mathbf{u}_{gw}$ (note that the superscript *"0"* denotes variables as they would be measured in the absence of groundwater flow; i.e., in the *"neutral state"*). The applicability of the first assumption will be context specific; e.g., it is more likely to apply during base flow than storm flow. The validity of assumption (2) will depend on whether or not the REA is large enough to encompass all of the hyporheic exchange flows of interest. For example, recent studies suggest that in-stream processing is dominated by hyporheic exchange through submerged bedforms, such as ripples, dunes, and riffle-pool sequences [*Gomez-Velez and Harvey*, 2014; *Gomez-Velez et al.*, 2015]. Thus, the REA should be large enough to capture hyporheic exchange across the largest of these bedform features, namely riffle-pool sequences. The third assumption should apply in the common case where the underlying equations governing hyporheic exchange are linear (for

Accepted Article

This article is protected by copyright. All rights reserved.

example the Laplace Equation for bedform pumping [*Boano et al.*, 2008]), but may not apply in cases where hyporheic exchange is driven primarily by momentum transfer across the sediment-water interface [*Boano et al.*, 2011], and pore water turnover associated with bedform migration [*Ahmerkamp et al.*, 2015]. Derivations for the results presented below can be found in the Supplemental Information.

2.2. Case 1: Neutral Stream

When there are no stream-groundwater interactions the thin film model parameters in equation (3a) reduce to $\gamma^0 = 1$ and $k_m^0 = \overline{u}_{SSE}^0$. The variable $\overline{u}_{SSE}^0$ represents the average Darcy flux across the sediment-water interface by hyporheic exchange (referred to here as *"small scale exchange"*, indicated by the subscript *"SSE"*) in the absence of regional scale groundwater flow (indicated by the superscript *"0"*).

$$J^0 = -\overline{u}_{SSE}^0 \left(C_{DW} - \overline{C}_{UW} \right) \tag{6}$$

When this result is translated into solute uptake velocity (see equation (5)), we find that v_f declines in proportion to the fraction of solute concentration that breaks through to the upwelling zone, $\overline{C}_{UW}/C_{DW}$ (line labeled *"Neutral"* in Figure 2). The solute uptake velocity equals the small scale exchange flux in the mass transfer limit ($v_f = \overline{u}_{SSE}^0$ when $\overline{C}_{UW} = 0$), and equals zero in the conservative solute limit ($v_f = 0$ when $\overline{C}_{UW} = C_{DW}$). While the solute uptake velocity is zero for the conservative solute limit (implying that there is no net mass flux across the sediment-water interface in this case), there can still be considerable gross mass flux across individual downwelling and upwelling zones. This distinction between net and gross mass flux also applies to the expressions derived below for losing and gaining streams.

Accepted Article

This article is protected by copyright. All rights reserved.

2.3. Case 2: Losing stream

When the stream is losing, mass transfer across the sediment-water interface is modified in a number of ways. Using the neutral case as a benchmark, our conceptual model implies that the losing condition affects the spatial distribution of upwelling and downwelling zones within the REA as follows (bottom panel, Figure 1): (1) intensifies the flux of water into the sediment bed over the original downwelling zone (bed surface area A^0_{DW}); (2) expands the downwelling zone to include areas that were previously neither upwelling nor downwelling (bed surface area A^0_N); (3) expands the downwelling zone to include an area that was previously occupied by an upwelling zone (bed surface area A^+_{DW}); and (4) diminishes the flux of water out of the upwelling zone (bed surface area A^-_{UW}). Taking these four adjustments into account, the thin film model parameters become $k^l_m = \overline{u}^l_{TOT}$ and $\gamma^l = \overline{u}^l_{SSE}/\overline{u}^l_{TOT}$:

$$J^l = -\overline{u}^l_{TOT}\left(C_{DW} - \frac{\overline{u}^l_{SSE}}{\overline{u}^l_{TOT}}\overline{C}_{UW}\right) \tag{7a}$$

$$\overline{u}^l_{TOT} = \overline{u}^l_{SSE} + \overline{u}_{gw} \tag{7b}$$

$$\overline{u}^l_{SSE} = \overline{u}^0_{SSE} - \overline{u}_{gw}\left(\frac{A^-_{UW} + \alpha A^+_{DW}}{\lambda P}\right) \tag{7c}$$

Variables appearing here include include the average flux of groundwater across the sediment-water interface ($\overline{u}_{gw}$, definition in Table 1 (equation (T1b)), the flux of water ($\overline{u}^l_{TOT}$) from the stream to the sediment in the expanded downwelling area ($A^0_{DW} + A^0_N + A^+_{DW}$), and the flux of water undergoing small-scale hyporheic exchange ($\overline{u}^l_{SSE}$) through the diminished upwelling area (A^-_{UW}). The superscript *"l"* denotes losing conditions, and the constant α is bounded between 0 and 1 (see definition in equation (T3c), Table 1); as will be shown in Section 4, α is well approximated by $\alpha = 0.5$.

Accepted Article

This article is protected by copyright. All rights reserved.

Relative to the neutral case, losing conditions favour mass transport into the streambed by two mechanisms: (1) the mass transfer coefficient increases (i.e., $k_m^l = \overline{u}_{TOT}^l > k_m^0 = \overline{u}_{SSE}^0$); and (2) the upwelling concentration is attenuated ($\gamma^l = \overline{u}_{SSE}^l / \overline{u}_{TOT}^l < 1$). Relative to point (1), the inequality $\overline{u}_{TOT}^l > \overline{u}_{SSE}^0$ can be demonstrated by substituting equations (7b) and (7c) for $\overline{u}_{TOT}^l$ and $\overline{u}_{SSE}^0$ respectively, and then noting that the following inequalities hold for $\alpha \in [0, 1]$: $A_{UW}^- + \alpha A_{DW}^+ \leq A_{DW}^0 < \lambda P$. Relative to point (2), groundwater flux can also alter subsurface chemical and physical conditions that control the fate of solutes undergoing hyporheic exchange, and hence the upwelling solute concentration $\overline{C}_{UW}$ may also change as the magnitude of $\overline{u}_{gw}$ increases (discussed further in Section 3).

Substituting k_m^l and γ^l into equation (5) we find that losing conditions: (1) increase v_f by increasing the loss of solute mass to groundwater (as manifest by an upward shift of the *"Losing"* line in Figure 2); and (2) decrease v_f by reducing the small scale exchange flux (see equation (7c)). The net impact of these two opposing processes on v_f will depend on the geometry of hyporheic exchange, as represented by the upwelling and downwelling areas in equation (7c).

2.4. Case 3: Gaining stream

The analysis for a gaining stream is similar to the case just discussed (Section 2.3), except for the direction of groundwater flow and the fact that groundwater itself may contribute solute mass to the stream. Benchmarked relative to the neutral case, the gaining condition (top panel, Figure 1): (1) intensifies the flux of water into the stream over the original upwelling zone (bed surface area A_{UW}^0); (2) expands the upwelling zone to include areas that were previously neither upwelling nor downwelling (bed surface area A_N^0); (3) expands the upwelling zone to include an area that was previously occupied by a

Accepted Article

This article is protected by copyright. All rights reserved.

downwelling zone (bed surface area A^+_{UW}); and (4) diminishes the flux of water out of what is left of the downwelling zone (bed surface area A^-_{DW}). After making these adjustments, the mass transport parameters become $k^g_m = \overline{u}^g_{SSE}$ and $\gamma^g = \overline{u}^g_{TOT}/\overline{u}^g_{SSE}$:

$$J^g = -\overline{u}^g_{SSE}\left(C_{DW} - \frac{\overline{u}^g_{TOT}}{\overline{u}^g_{SSE}}\overline{C}_{UW}\right) \tag{8a}$$

$$\overline{u}^g_{TOT} = \overline{u}^g_{SSE} + \overline{u}_{gw} \tag{8b}$$

$$\overline{u}^g_{SSE} = \overline{u}^0_{SSE} - \overline{u}_{gw}\left(\frac{A^-_{DW} + \beta A^+_{UW}}{\lambda P}\right) \tag{8c}$$

The variables appearing here have the same meaning as in the previous section, except that the superscript *"g"* refers to gaining conditions and the constant β is bounded by 0 and 1; as will be shown later, β is well approximated by 0.5 (see definition in equation (T4c), Table 1).

Relative to the neutral case, gaining conditions favour solute transport into the stream by three mechanisms: (1) the mass transfer constant is reduced ($k^g_m = \overline{u}^g_{SSE} < k^0_m = \overline{u}^0_{SSE}$) which reduces the mass transfer limited flux ($J^g_{MTL} = -k^g_m C_{DW}$) into the sediment bed; (2) the heavier weighting of the upwelling concentration ($\gamma^g = \overline{u}^g_{TOT}/\overline{u}^g_{SSE} > 1$) leads to a more positive mass flux all else being equal (recall that when $J < 0$ the net solute flux is into the sediment bed); and (3) the flow-weighted upwelling concentration ($\overline{C}_{UW}$) will increase when groundwater has a non-zero concentration of solute. The inequalities $\overline{u}^g_{SSE} < \overline{u}^0_{SSE}$ and $\overline{u}^g_{TOT} > \overline{u}^0_{SSE}$ can be demonstrated by substituting equations (8b) and (8c) for $\overline{u}^g_{TOT}$ and $\overline{u}^g_{SSE}$, respectively.

Substituting k^g_m and γ^g into equation (5) we find that gaining conditions: (1) reduce v_f by decreasing the small scale exchange flux (equation 8c); and (2) cause v_f to decline more quickly as the normalised breakthrough concentration increases, reflecting the fact

Accepted Article

This article is protected by copyright. All rights reserved.

that $\gamma^g > 1$ in equation (8) (see line labeled *"Gaining"* in Figure 2). If the groundwater contains solute, then the value of the solute uptake velocity is reduced further by the quotient $u_{gw} \cdot C_{gw}/C_{DW}$, where C_{gw} is the solute concentration in the groundwater (all other terms have been defined previously).

3. Upwelling Solute Concentration and Hyporheic Zone RTD

In the last section we demonstrated that a modified form of the thin film model describes mass transport across the sediment-water interface by hyporheic exchange in neutral, gaining, and losing streams. A key variable in our thin film model is the breakthrough concentration in the upwelling zone, $\overline{C}_{UW}$. Here we focus on a surprising duality associated with the calculation of $\overline{C}_{UW}$; namely, it can be represented as a flow-weighted average over the upwelling zone (see equation (3b)) or as a convolution over the RTD of water parcels in the hyporheic zone [*Azizian et al.*, 2015]:

$$\overline{C}_{UW}(t) = \int_0^\infty C_{UW}(t|\tau)\, E(\tau)\, d\tau \tag{9}$$

New variables appearing in equation (9) include the time (τ) it takes stream water to transit along a particular streamline through the hyporheic zone and the probability density function of the hyporheic zone RTD ($E(\tau) = dF_{RTD}/d\tau$). The notation $C_{UW}(t|\tau)$ refers to the upwelling solute concentration at time t on a streamline of residence time τ. The functional dependence of $C_{UW}(t|\tau)$ on t and τ could arise in several ways: (1) unsteadiness associated with the solute concentration in the stream because solute emerging from the upwelling zone entered the downwelling zone some time earlier; (2) physicochemical or biogeochemical reactions that influence the production or loss of solute in the sediment (such as nitrification or denitrification in the case of nitrate); and/or (3)

Accepted Article

This article is protected by copyright. All rights reserved.

mixing with ambient groundwater that has a chemical signature different from that of the stream water. As an example, if a time varying solute concentration in a stream reach ($C_w(t)$) is coupled with removal by first-order reaction in the sediment (and assuming no solute mixing in the sediment by molecular diffusion or mechanical dispersion), the concentration term in equation (9) becomes $C_{UW}(t|\tau) = C_w(t-\tau)\,e^{-\kappa\tau}$, where κ is the first order rate constant [*Dagan et al.*, 1992; *Cvetkovic and Dagan*, 1994; *Grant et al.*, 2014; *Azizian et al.*, 2015]. Because $\overline{C}_{UW}$ is required to calculate the benthic flux J (see equations (6), (7a), and (8a)), equation (9) bridges three complementary approaches for modelling solute transport in streams with hyporheic zones: random walk descriptions which require specification of the RTD function $E(\tau) = dF_{RTD}/d\tau$, advection-dispersion equations that require specification of J, and stream network model descriptions that require the specification of $v_f = -J/C_{DW}$.

4. Testing the Thin Film Model for Hyporheic Exchange

In this section we test our thin film model against three previously published studies of hyporheic exchange with stream-groundwater interactions under neutral, losing and/or gaining conditions: (1) an analytical study of hyporheic exchange across fluvial ripples; (2) a laboratory study of hyporheic exchange across ripples; and (3) numerical simulations of hyporheic exchange across a fully submerged three-dimensional riffle-pool sequence. As will be shown, in all of these test cases the thin film model correctly describes how small-scale exchange responds to ambient groundwater flux and the areal extents of upwelling and downwelling zones within an REA. While the thin film model correctly diagnosis the relationship between these variables, being a kinematic analysis it cannot predict their

Accepted Article

This article is protected by copyright. All rights reserved.

magnitudes without additional information, for example, from physically based models or experimental measurements.

4.1. Hyporheic Exchange Across Fluvial Ripples

Boano and co-authors [2008; 2009] developed an analytical model of hyporheic exchange across fluvial ripples under the influence of stream-groundwater interactions. The authors modified a simple analytical model for hyporheic exchange (the *Advective Pumping Model* (APM) developed by *Elliott and Brooks* [1997a]) to account for vertical groundwater flux. Adopting the APM for local small-scale exchange, the Darcy flux at the sediment-water interface can be written as follows:

$$\mathbf{u}_{hz}^{0} \cdot \hat{\mathbf{n}} = -u_m \sin(kx) \tag{10a}$$

$$u_m = kK_h h_m \tag{10b}$$

$$k = 2\pi/\lambda \tag{10c}$$

New variables include the streamwise coordinate (x), a characteristic velocity scale for the hyporheic flow across a bedform (u_m), the bedform wavenumber (k), the bedform wavelength (λ), the maximum dynamic pressure head perturbation caused by the presence of the bedform (h_m), and the hydraulic conductivity of the sediment (K_h). For this model, the REA is of dimensions $\lambda \times P$, where (as we noted earlier) P is the width of the stream. Substituting equation (10a) into our definition of $\overline{u}_{SSE}^{0}$ (equation (T2a) in Table 1) and integrating over a single downwelling zone ($A_{DW}^{0} = Px$ where $0 \leq x \leq \lambda/2$) we obtain the well-known result for the average Darcy flux produced by hyporheic exchange across two-dimensional bedforms under neutral conditions (i.e., SSE in the absence of stream-groundwater interactions): $\overline{u}_{SSE}^{0} = u_m/\pi$. According to *Boano et al.'s* analysis, under

Accepted Article

This article is protected by copyright. All rights reserved.

gaining conditions the downwelling area contracts ($A^{-}_{DW} = \frac{\lambda P}{2}\left(1 - \frac{2}{\pi} sin^{-1}\overline{u}_{up}\right)$) and the upwelling area expands ($A^{+}_{UW} = \frac{\lambda P}{\pi} sin^{-1}\overline{u}_{up}$), where the vertical groundwater flux is reduced as follows: $\overline{u}_{up} = u_{gw}/u_m$ [*Boano et al.*, 2009]. Substituting these results into equation (8c) yields our prediction for the average small scale exchange under gaining conditions (see Supplemental Information for details):

$$\overline{u}^{g}_{SSE} = \overline{u}^{0}_{SSE} - \overline{u}_{gw}\left(\frac{1}{2} - \frac{sin^{-1}\overline{u}_{up}}{\pi} + \frac{1 - \sqrt{1 - \overline{u}^{2}_{up}}}{\pi \overline{u}_{up}}\right) \tag{11}$$

Boano et al. [2009] defined the normalised small-scale exchange flux as follows: $q^{*}_{SSE} = \overline{u}^{g}_{SSE}/\pi\overline{u}^{0}_{SSE}$. Substituting equation (11) we recover *Boano et al's* theoretical result for reduced small scale exchange flux (equation (14) in their paper):

$$q^{*}_{SSE} = \frac{\overline{u}_{up}}{\pi} sin^{-1}\overline{u}_{up} + \frac{1}{\pi}\sqrt{1 - \overline{u}^{2}_{up}} - \frac{\overline{u}_{up}}{2} \tag{12}$$

We can also derive from *Boano et al.'s* analytical solution an explicit expression for the constant β appearing in equation (8c). Under gaining conditions, the expanded upwelling area A^{+}_{UW} is associated with the following two intervals along the x-axis: $kx \in \left(0, \sin^{-1}\overline{u}_{up}\right) \cup \left(\pi - \sin^{-1}\overline{u}_{up}, \pi\right)$. Integrating the definition of β over these two intervals (see equation (T4c), Table 1) we obtain the following result:

$$\beta = \frac{1 - \sqrt{1 - \overline{u}^{2}_{up}}}{\overline{u}_{up} \sin^{-1}\overline{u}_{up}} \tag{13}$$

Equation (13) predicts that β varies from 0.5 in the absence of stream-groundwater interactions ($\overline{u}_{up} = 0$) to $2/\pi \approx 0.64$ when the groundwater flux overwhelms hyporheic exchange ($\overline{u}_{up} \geq 1$). The functional dependence of β on $\overline{u}_{up}$ is illustrated in Figure 3 (blue dotted curve).

Accepted Article

This article is protected by copyright. All rights reserved.

4.2. Experimental Measurements of Hyporheic Exchange

Next we applied our thin film model to previously published experimental measurements of hyporheic exchange across ripples under gaining, neutral, and losing conditions [*Fox et al.*, 2014]. These experiments were conducted by adding a pulse of conservative dye to the water phase of a recirculating flume and then measuring the mass flux of dye into the sediment bed (which was shaped into artificial ripples) over time. We compared *Fox et al.'s* experimentally determined Darcy fluxes ($\overline{u}^l_{TOT}$, $\overline{u}^l_{SSE}$, $\overline{u}^g_{TOT}$, and $\overline{u}^g_{SSE}$) to the corresponding values estimated from our thin film model (equations (7b), (7c), (8b) and (8c)), using experimental values of $\overline{u}^0_{SSE}$ reported by *Fox et al.* [2014], observed downwelling and upwelling areas (visualised by dye in *Fox et al's* experiments), and setting $\alpha = \beta = 0.5$ (see further discussion of this assumption in Section 4.3). It should be noted that *Fox et al.* reported two sets of values for $\overline{u}^0_{SSE}$: one set that was directly measured by performing mass balance on dye added to the flume (see equation (7) in their paper) and another set calculated from *Boano et al.'s* theoretical model (see Section 4.1). Here we utilised the experimentally determined values of $\overline{u}^0_{SSE}$; to do otherwise would amount to another test of *Boano et al.'s* model. As illustrated in Figure 4, our thin film model-predicted Darcy fluxes compare favourably with the corresponding experimental values reported by *Fox et al.* (blue symbols, Figure 4).

4.3. Hyporheic Exchange Across Riffle-Pool Sequences

As a final test, we compared our thin film model with previously published computational fluid dynamic (CFD) simulations of hyporheic exchange across three-dimensional and fully submerged riffle-pool sequences. *Trauth et al.* [2013] carried out sixty-six CFD simulations of turbulent surface flow over an idealised riffle-pool bedform topography (il-

Accepted Article

This article is protected by copyright. All rights reserved.

lustrated in Figure 5a). From the CFD-predicted pressure variations over the sediment surface, these authors calculated the hyporheic exchange flow field through the sediments from Darcy's Law and the continuity equation. Simulations were carried out for a range of Re (from $10^{5.95}$ to $10^{6.52}$) and different groundwater exchange rates, including six neutral conditions and 30 gaining and losing conditions (± 0.5, ± 1.0, ± 1.5, ± 2.0 and ± 2.5 $cm \cdot day^{-1}$ for each of the six Re values). We used the thin film model (specifically, equations (7c) and (8c)) to estimate small-scale exchange fluxes for all of *Trauth et al.s* simulations. This involved three steps. First, for each Re we computed a value for $\overline{u}^0_{SSE}$ by integrating the simulated velocity field at the sediment-water interface $\mathbf{u}^0_{hz}$ over a downwelling zone under neutral conditions (see equation (T2a) in Table 1). An example of the simulated velocity field $\mathbf{u}^0_{hz}$ is shown in Figure (5a). Second, we evaluated how the upwelling and downwelling areas: (1) expand (A^+_{UW}) and contract (A^-_{DW}) under gaining conditions; and (2) contract (A^-_{UW}) and expand (A^+_{DW}) under losing conditions. This step is illustrated in Figure (5) for losing (Figure (5b)), neutral (Figure (5c)), and gaining (Figure (5d)) conditions. Finally, the results from the first two steps were substituted into equations (7c) and (8c) to obtain estimates for the small-scale exchange flux under gaining ($\overline{u}^g_{SSE}$) and losing ($\overline{u}^l_{SSE}$) conditions, assuming an REA of 50 m^2 ($\lambda = 10$ m, $P = 5$ m) and $\alpha = \beta = 0.5$. The small scale exchange fluxes obtained by this approach agree well with the hyporheic exchange fluxes reported by *Trauth et al.* [2013] (red symbols, Figure 4). We also calculated from *Trauth et al.'s* simulated velocity fields values of α and β (by numerically integrating equations (T3c) and (T4c) respectively, Table 1). These calculations confirm that $\alpha \approx \beta \approx 0.5$; specifically, when averaged across all of *Trauth et al.'s* simulations we obtain $\alpha = 0.48 \pm 0.04$, $\beta = 0.45 \pm 0.08$ (see asterisks in Figure

Accepted Article

This article is protected by copyright. All rights reserved.

3). In summary, regardless of whether mass transfer is simulated (e.g., using the APM or numerical methods) or measured (e.g., *Fox et al.* [2014]), our thin film model accurately forecasts how small scale hyporheic exchange fluxes (and by inference the solute uptake velocity, see equation (5)) change in response to gaining and losing conditions.

5. Conclusions

In this study we employed simple kinematic arguments to derive a thin film model for mass transfer across the sediment-water interface by hyporheic exchange in gaining, neutral, or losing streams. In our variant of the thin film model, the mass transfer coefficient is the average downwelling Darcy flux of water, and the driving force for mass transfer is the weighted difference between mass concentrations on the stream-side of the downwelling zone and sediment-side of the upwelling zone. Gaining or losing conditions affect mass flux in two ways: (1) by reducing the flux of water circulating between downwelling and upwelling zones (small-scale exchange); and (2) by altering the flow-weighted concentration in the upwelling zone. Our thin film model reproduces previously derived expressions for small-scale exchange across fluvial ripples coupled with vertical groundwater flux, after incorporating the geometric constraints on groundwater-surface water mixing of *Boano et al.* [2008, 2009]. It is also consistent with experimental flume measurements of hyporheic exchange under losing, neutral, and gaining conditions, together with CFD simulations of hyporheic exchange across three-dimensional riffle-pool sequences. Finally, our theory bridges three complementary approaches for modelling hyporheic exchange in rivers, including random walk approaches that rely on the specification of an encounter frequency and an RTD function for wait times in the hyporheic zone, advection-dispersion models that rely on specification of mass flux across the sediment-water interface, and stream

Accepted Article

This article is protected by copyright. All rights reserved.

network models that rely on specification of the solute uptake velocity within each reach of the network. By expanding previous analyses to a broad range of geometries and hyporheic exchange mechanisms (including hyporheic exchange driven by both dynamic and static pressure variations over the sediment-water interface), the kinematic framework developed here should support ongoing efforts to better understand how fluvial ecosystem services (such as respiration, nitrification, and denitrification) are affected by changes in regional groundwater hydrology associated with urbanisation, agricultural activities, groundwater extraction, and climate change.

Acknowledgments. Data presented in Figures 4 and 5 is either properly cited and referred to in the reference list, or was calculated from data kindly provided by A. Fox and N. Trauth. We also thank B. Cardenas, A. Sawyer, S Stonedahl, J. Harvey and the following individuals for their detailed review of the manuscript: M. Azizian, C. Berni, R. Casas-Mulet, E. Gee, A. Herrero, D. O'Shea and M. Rippy. Financial support was provided by the Australian Government through an Australian Postgraduate Award, the Australian Research Council Development Project Grant (DP-130103619) and the U.S. National Science Foundation Partnerships for International Research and Education (PIRE) (OISE-1243543).

References

Ahmerkamp, S., C. Winter, F. Janssen, M. M. M. Kuypers, and M. Holtappels (2015), The impact of bedform migration on benthic oxygen fluxes, *Journal of Geophysical Research: Biogeosciences*, pp. n/a–n/a, doi:10.1002/2015JG003106.

Accepted Article

This article is protected by copyright. All rights reserved.

Aubeneau, A. F., J. D. Drummond, R. Schumer, D. Bolster, J. L. Tank, and A. I. Packman (2015), Effects of benthic and hyporheic reactive transport on breakthrough curves, *Freshwater Science*, *34*.

Azizian, M., S. B. Grant, A. J. Kessler, P. L. M. Cook, M. A. Rippy, and M. J. Stewardson (2015), Bedforms as biocatalytic filters: A pumping and streamline segregation model for nitrate removal in permeable sediments, *Environmental Science & Technology*, doi: 10.1021/acs.est.5b01941.

Bardini, L., F. Boano, M. B. Cardenas, R. Revelli, and L. Ridolfi (2012), Nutrient cycling in bedform induced hyporheic zones, *Geochimica et Cosmochimica Acta*, *84*(0), 47–61.

Bear, J., and A. H.-D. Cheng (2010), *Modeling groundwater flow and contaminant transport*, vol. 23, Springer Science & Business Media.

Bencala, K. E., and R. A. Walters (1983), Simulation of solute transport in a mountain poolandriffle stream with a kinetic mass transfer model for sorption, *Water Resources Research*, *19*(3), 732–738.

Boano, F., A. I. Packman, A. Cortis, R. Revelli, and L. Ridolfi (2007), A continuous time random walk approach to the stream transport of solutes, *Water Resources Research*, *43*(10), W10,425, doi:10.1029/2007WR006062.

Boano, F., R. Revelli, and L. Ridolfi (2008), Reduction of the hyporheic zone volume due to the stream-aquifer interaction, *Geophysical Research Letters*, *35*(9), n/a–n/a, doi:10.1029/2008GL033554.

Boano, F., R. Revelli, and L. Ridolfi (2009), Quantifying the impact of groundwater discharge on the surfacesubsurface exchange, *Hydrological Processes*, *23*(15), 2108–2116, doi:10.1002/hyp.7278.

Accepted Article

This article is protected by copyright. All rights reserved.

Boano, F., R. Revelli, and L. Ridolfi (2011), Water and solute exchange through flat streambeds induced by large turbulent eddies, *Journal of Hydrology*, *402*(3-4), 290–296.

Boano, F., J. W. Harvey, A. Marion, A. I. Packman, R. Revelli, L. Ridolfi, and A. Wrman (2014), Hyporheic flow and transport processes: Mechanisms, models, and biogeochemical implications, *Reviews of Geophysics*, p. 2012RG000417.

Briggs, M. A., F. D. Day-Lewis, J. P. Zarnetske, and J. W. Harvey (2015), A physical explanation for the development of redox microzones in hyporheic flow, *Geophysical Research Letters*, *42*(11), 4402–4410, doi:10.1002/2015GL064200.

Cardenas, M. B. (2015), Hyporheic zone hydrologic science: a historical account of its emergence and a prospectus, *Water Resources Research*, pp. n/a–n/a, doi:10.1002/2015WR017028.

Cardenas, M. B., and J. L. Wilson (2007), Hydrodynamics of coupled flow above and below a sedimentwater interface with triangular bedforms, *Advances in Water Resources*, *30*(3), 301–313.

Cardenas, M. B., J. L. Wilson, and R. Haggerty (2008), Residence time of bedform-driven hyporheic exchange, *Advances in Water Resources*, *31*(10), 1382–1386.

Cussler, E. L. (2009), *Diffusion: mass transfer in fluid systems*, Cambridge university press.

Cvetkovic, V., and G. Dagan (1994), Transport of kinetically sorbing solute by steady random velocity in heterogeneous porous formations, *Journal of Fluid Mechanics*, *265*, 189–215, doi:doi:10.1017/S0022112094000807.

Accepted Article

This article is protected by copyright. All rights reserved.

Dagan, G., V. Cvetkovic, and A. Shapiro (1992), A solute flux approach to transport in heterogeneous formations: 1. the general framework, *Water Resources Research*, *28*(5), 1369–1376, doi:10.1029/91WR03086.

Deng, Z.-Q., V. P. Singh, and L. Bengtsson (2004), Numerical solution of fractional advection-dispersion equation, *Journal of Hydraulic Engineering*, *130*(5), 422–431, doi: doi:10.1061/(ASCE)0733-9429(2004)130:5(422).

Elliott, A. H., and N. H. Brooks (1997a), Transfer of nonsorbing solutes to a streambed with bed forms: Theory, *Water Resources Research*, *33*(1), 123–136.

Elliott, A. H., and N. H. Brooks (1997b), Transfer of nonsorbing solutes to a streambed with bed forms: Laboratory experiments, *Water Resour. Res.*, *33*(1), 137–151.

Fox, A., F. Boano, and S. Arnon (2014), Impact of losing and gaining streamflow conditions on hyporheic exchange fluxes induced by dune-shaped bed forms, *Water Resources Research*, *50*(3), 1895–1907.

Gomez-Velez, J. D., and J. W. Harvey (2014), A hydrogeomorphic river network model predicts where and why hyporheic exchange is important in large basins, *Geophysical Research Letters*, *41*(18), 6403–6412, doi:10.1002/2014GL061099.

Gomez-Velez, J. D., J. W. Harvey, M. B. Cardenas, and B. Kiel (2015), Denitrification in the mississippi river network controlled by flow through river bedforms, *Nature Geosci*, *8*(12), 941–945, doi:10.1038/ngeo2567.

González-Pinzón, R., A. S. Ward, C. E. Hatch, A. N. Wlostowski, K. Singha, M. N. Gooseff, R. Haggerty, J. W. Harvey, O. A. Cirpka, and J. T. Brock (2015), A field comparison of multiple techniques to quantify groundwater-surface-water interactions, *Freshwater Science*, *34*(1), 139–160, doi:10.1086/679738.

Accepted Article

This article is protected by copyright. All rights reserved.

Gooseff, M. N., R. O. Hall, and J. L. Tank (2007), Relating transient storage to channel complexity in streams of varying land use in jackson hole, wyoming, *Water Resources Research*, *43*(1).

Grant, S. B., and I. Marusic (2011), Crossing turbulent boundaries: Interfacial flux in environmental flows, *Environmental Science & Technology*, *45*(17), 71077113.

Grant, S. B., M. J. Stewardson, and I. Marusic (2012), Effective diffusivity and mass flux across the sediment-water interface in streams, *Water Resources Research*, *48*(5), W05,548.

Grant, S. B., K. Stolzenbach, M. Azizian, M. J. Stewardson, F. Boano, and L. Bardini (2014), First-order contaminant removal in the hyporheic zone of streams: Physical insights from a simple analytical model, *Environmental Science & Technology*, *48*(19), 11,369–11,378.

Haggerty, R., S. M. Wondzell, and M. A. Johnson (2002), Power-law residence time distribution in the hyporheic zone of a 2nd-order mountain stream, *Geophysical Research Letters*, *29*(13), 18–1–18–4, doi:10.1029/2002GL014743.

Harvey, J., and M. Gooseff (2015), River corridor science: Hydrologic exchange and ecological consequences from bedforms to basins, *Water Resources Research*, *51*(9), 6893–6922, doi:10.1002/2015WR017617.

Herzog, S., C. Higgins, and J. McCray (2015), Engineered streambeds for induced hyporheic flow: Enhanced removal of nutrients, pathogens, and metals from urban streams, *Journal of Environmental Engineering*, *0*(0), 04015,053, doi: doi:10.1061/(ASCE)EE.1943-7870.0001012.

Accepted Article

This article is protected by copyright. All rights reserved.

Hester, E. T., and M. N. Gooseff (2010), Moving beyond the banks: Hyporheic restoration is fundamental to restoring ecological services and functions of streams, *Environmental Science & Technology*, *44*(5), 1521–1525.

Hester, E. T., K. I. Young, and M. A. Widdowson (2013), Mixing of surface and groundwater induced by riverbed dunes: Implications for hyporheic zone definitions and pollutant reactions, *Water Resources Research*, *49*(9), 5221–5237, doi:10.1002/wrcr.20399.

Hinkle, S. R., J. H. Duff, F. J. Triska, A. Laenen, E. B. Gates, K. E. Bencala, D. A. Wentz, and S. R. Silva (2001), Linking hyporheic flow and nitrogen cycling near the Willamette River - a large river in Oregon, USA, *Journal of Hydrology*, *244*(34), 157–180, doi:http://dx.doi.org/10.1016/S0022-1694(01)00335-3.

Kessler, A. J., R. N. Glud, M. B. Cardenas, M. Larsen, M. F. Bourke, and P. L. M. Cook (2012), Quantifying denitrification in rippled permeable sands through combined flume experiments and modeling, *Limnology and Oceanography*, *57*(4), 1217–1232, doi:10.4319/lo.2012.57.4.1217.

Kiel, B. A., and M. B. Cardenas (2014), Lateral hyporheic exchange throughout the mississippi river network, *Nature Geoscience*, *7*(6), 413–417.

Krause, S., D. M. Hannah, J. H. Fleckenstein, C. M. Heppell, D. Kaeser, R. Pickup, G. Pinay, A. L. Robertson, and P. J. Wood (2011), Inter-disciplinary perspectives on processes in the hyporheic zone, *Ecohydrology*, *4*(4), 481–499.

Marion, A., M. Zaramella, and A. Bottacin-Busolin (2008), Solute transport in rivers with multiple storage zones: The stir model, *Water Resources Research*, *44*(10), n/a–n/a, doi:10.1029/2008WR007037.

Accepted Article

This article is protected by copyright. All rights reserved.

Marzadri, A., D. Tonina, and A. Bellin (2011), A semianalytical three-dimensional process-based model for hyporheic nitrogen dynamics in gravel bed rivers, *Water Resources Research*, *47*(11), n/a–n/a, doi:10.1029/2011WR010583.

Marzadri, A., D. Tonina, A. Bellin, and J. L. Tank (2014), A hydrologic model demonstrates nitrous oxide emissions depend on streambed morphology, *Geophysical Research Letters*, *41*(15), 5484–5491, doi:10.1002/2014GL060732.

Mulholland, P. J., A. M. Helton, G. C. Poole, R. O. Hall, S. K. Hamilton, B. J. Peterson, J. L. Tank, L. R. Ashkenas, L. W. Cooper, C. N. Dahm, W. K. Dodds, S. E. G. Findlay, S. V. Gregory, N. B. Grimm, S. L. Johnson, W. H. McDowell, J. L. Meyer, H. M. Valett, J. R. Webster, C. P. Arango, J. J. Beaulieu, M. J. Bernot, A. J. Burgin, C. L. Crenshaw, L. T. Johnson, B. R. Niederlehner, J. M. O/'Brien, J. D. Potter, R. W. Sheibley, D. J. Sobota, and S. M. Thomas (2008), Stream denitrification across biomes and its response to anthropogenic nitrate loading, *Nature*, *452*(7184), 202–205, 10.1038/nature06686.

Nordin, C. F., and B. M. Troutman (1980), Longitudinal dispersion in rivers: The persistence of skewness in observed data, *Water Resources Research*, *16*(1), 123–128.

O'Connor, B. L., and M. Hondzo (2008), Dissolved oxygen transfer to sediments by sweep and eject motions in aquatic environments, *Limnology and Oceanography*, *53*(2), 566–578.

Packman, A. I., N. H. Brooks, and J. J. Morgan (2000), Kaolinite exchange between a stream and streambed: Laboratory experiments and validation of a colloid transport model, *Water Resources Research*, *36*(8), 2363–2372.

Potter, M. C., D. C. Wiggert, M. Hondso, and T. I.-P. Shih (2012), *Mechanics of Fluids*, vol. 4th, Brooks/Cole, Pacific Grove, CA, USA, pp. 132–136.

Accepted Article

This article is protected by copyright. All rights reserved.

Pryshlak, T. T., A. H. Sawyer, S. H. Stonedahl, and M. R. Soltanian (2015), Multiscale hyporheic exchange through strongly heterogeneous sediments, *Water Resources Research*, *51*(11), 9127–9140, doi:10.1002/2015WR017293.

Ren, J., and A. I. Packman (2004), Stream-subsurface exchange of zinc in the presence of silica and kaolinite colloids, *Environmental Science & Technology*, *38*(24), 6571–6581.

Runkel, R. L. (1998), One-dimensional transport with inflow and storage (otis): A solute transport model for streams and rivers.

Schumer, R., D. A. Benson, M. M. Meerschaert, and B. Baeumer (2003), Fractal mobile/immobile solute transport, *Water Resources Research*, *39*(10), n/a–n/a, doi:10.1029/2003WR002141.

Stonedahl, S. H., J. W. Harvey, A. Wrman, M. Salehin, and A. I. Packman (2010), A multiscale model for integrating hyporheic exchange from ripples to meanders, *Water Resources Research*, *46*(12), n/a–n/a, doi:10.1029/2009WR008865.

Stonedahl, S. H., J. W. Harvey, and A. I. Packman (2013), Interactions between hyporheic flow produced by stream meanders, bars, and dunes, *Water Resources Research*, *49*(9), 5450–5461, doi:10.1002/wrcr.20400.

Storey, R. G., K. W. F. Howard, and D. D. Williams (2003), Factors controlling riffle-scale hyporheic exchange flows and their seasonal changes in a gaining stream: A three-dimensional groundwater flow model, *Water Resour. Res.*, *39*(2), 1034.

Stream Solute Workshop (1990), Concepts and methods for assessing solute dynamics in stream ecosystems, *Journal of the North American Benthological Society*, *9*(2), 95–119, iSI Document Delivery No.: DP187 Times Cited: 139 Cited Reference Count: 0 AUMEN, NG Grimm, Nancy/D-2840-2009 Grimm, Nancy/0000-0001-9374-660X 141

Accepted Article

This article is protected by copyright. All rights reserved.

NORTH AMER BENTHOLOGICAL SOC LAWRENCE J N AM BENTHOL SOC.

Trauth, N., C. Schmidt, U. Maier, M. Vieweg, and J. H. Fleckenstein (2013), Coupled 3-d stream flow and hyporheic flow model under varying stream and ambient groundwater flow conditions in a pool-riffle system, *Water Resources Research*, *49*(9), 5834–5850, doi:10.1002/wrcr.20442.

Woessner, W. W. (2000), Stream and fluvial plain ground water interactions: Rescaling hydrogeologic thought, *Ground Water*, *38*(3), 423–429, doi:10.1111/j.1745-6584.2000.tb00228.x.

Wollheim, W. M., C. J. Vrsmarty, B. J. Peterson, S. P. Seitzinger, and C. S. Hopkinson (2006), Relationship between river size and nutrient removal, *Geophysical Research Letters*, *33*(6), n/a–n/a, doi:10.1029/2006GL025845.

Wörman, A., A. I. Packman, H. Johansson, and K. Jonsson (2002), Effect of flow-induced exchange in hyporheic zones on longitudinal transport of solutes in streams and rivers, *Water Resources Research*, *38*(1), 2–1–2–15, doi:10.1029/2001WR000769.

Wörman, A., A. I. Packman, L. Marklund, J. W. Harvey, and S. H. Stone (2006), Exact three-dimensional spectral solution to surface-groundwater interactions with arbitrary surface topography, *Geophysical Research Letters*, *33*(7), doi:10.1029/2006GL025747.

Wörman, A., A. I. Packman, L. Marklund, J. W. Harvey, and S. H. Stone (2007), Fractal topography and subsurface water flows from fluvial bedforms to the continental shield, *Geophysical Research Letters*, *34*(7), n/a–n/a, doi:10.1029/2007GL029426.

Accepted Article

This article is protected by copyright. All rights reserved.

Table 1. Thin film model results for neutral, gaining and losing conditions (all derivations provided in Supplemental Information).

Definitions of Key Variables for the thin film model of hyporheic exchange

$$\mathbf{v}_{SWI} = \mathbf{u}^{o}_{hz} + \mathbf{u}_{gw} \tag{T1a}$$

$$\overline{u}_{gw} = \frac{1}{A}\left|\int_{A} \mathbf{u}_{gw}\cdot\hat{\mathbf{n}}dA\right| \tag{T1b}$$

Small Scale Exchange (SSE) and Total Exchange (TOT) for neutral conditions

$$\overline{u}^{0}_{SSE} = -\frac{1}{\lambda P}\int_{A^{0}_{DW}} \mathbf{u}^{0}_{hz}\cdot\hat{\mathbf{n}}dA = \frac{1}{\lambda P}\int_{A^{0}_{UW}} \mathbf{u}^{0}_{hz}\cdot\hat{\mathbf{n}}dA \tag{T2a}$$

$$\overline{u}^{0}_{TOT} = \overline{u}^{0}_{SSE} \tag{T2b}$$

Small Scale Exchange (SSE) and Total Exchange (TOT) for losing conditions

$$\overline{u}^{l}_{SSE} = \frac{1}{\lambda P}\int_{A^{-}_{UW}} (\mathbf{u}^{0}_{hz} + \mathbf{u}_{gw})\cdot\hat{\mathbf{n}}dA = \overline{u}^{0}_{SSE} - \overline{u}_{gw}\left(\frac{A^{-}_{UW}+\alpha A^{+}_{DW}}{\lambda P}\right) \tag{T3a}$$

$$\overline{u}^{l}_{TOT} = \overline{u}^{l}_{SSE} + \overline{u}_{gw} \tag{T3b}$$

$$\alpha = \frac{1}{\overline{u}_{gw}A^{+}_{DW}}\int_{A^{+}_{DW}} \mathbf{u}^{0}_{hz}\cdot\hat{\mathbf{n}}dA, 0 \le \alpha \le 1 \tag{T3c}$$

$$\overline{u}^{l}_{SSE}, \overline{u}^{l}_{TOT}, \overline{u}_{gw} \ge 0 \tag{T3d}$$

Small Scale Exchange (SSE) and Total Exchange (TOT) for gaining conditions

$$\overline{u}^{g}_{SSE} = -\frac{1}{\lambda P}\int_{A^{-}_{DW}} (\mathbf{u}^{0}_{hz} + \mathbf{u}_{gw})\cdot\hat{\mathbf{n}}dA = \overline{u}^{0}_{SSE} - \overline{u}_{gw}\left(\frac{A^{-}_{DW}+\beta A^{+}_{UW}}{\lambda P}\right) \tag{T4a}$$

$$\overline{u}^{g}_{TOT} = \overline{u}^{g}_{SSE} + \overline{u}_{gw} \tag{T4b}$$

$$\beta = -\frac{1}{\overline{u}_{gw}A^{+}_{UW}}\int_{A^{+}_{UW}} \mathbf{u}^{0}_{hz}\cdot\hat{\mathbf{n}}dA, 0 \le \beta \le 1 \tag{T4c}$$

$$\overline{u}^{g}_{SSE}, \overline{u}^{g}_{TOT}, \overline{u}_{gw} \ge 0 \tag{T4d}$$

Accepted Article

This article is protected by copyright. All rights reserved.

Figure 1. Middle Panel: Plan view of a representative elemental area (REA) with dimensions of stream width (P) and length (λ) that contains arbitrarily shaped upwelling areas (*"UW"*, denoted by red area), downwelling areas (*"DW"*, denoted by blue area), or areas that are neither upwelling nor downwelling (*"N"*, denoted by white area) assuming no regional groundwater seepage (i.e., neutral stream, denoted by the superscript *"0"*). *"RTD"* refers to the residence time distribution of water in the hyporheic zone. Top and Bottom panels: stream-groundwater interactions affect the geometry of hyporheic exchange. Areas associated with upwelling and downwelling zones expand (superscript *"+"*), contract (superscript *"-"*), or remain the same (superscript *"0"*) going from neutral to gaining (upper panel) or from neutral to losing (lower panel) conditions.

Figure 2. Relationship between the normalised solute uptake velocity ($v_f/\overline{u}_{SSE}$) and the normalised breakthrough concentration of solute in an upwelling zone ($\overline{C}_{UW}/C_{DW}$) under neutral, losing, or gaining conditions (lines calculated from equation (5)).

Figure 3. Values of α and β derived from the Advective Pumping Model (dashed blue line) or estimated (asterisks) by integrating equations (T3c) and (T4c) (see Table 1) using *Trauth et al.'s* simulated velocity field (see main text).

Accepted Article

This article is protected by copyright. All rights reserved.

Figure 4. Comparison of normalised small-scale exchange (SSE) fluxes ($\overline{u}_{SSE}/\overline{U}$) calculated using the kinematic approach outlined in this study, plotted agains previously published values by *Fox et al.* [2014] (in blue) and *Trauth et al.* [2013] (in red), where $\overline{U}$ is the mean stream velocity.

Figure 5. Panel (a): Bedform topography of the idealised riffle-pool sequence employed by *Trauth et al.* [2013] in their CFD simulations; the vectors indicate one of the simulated velocity fields under neutral conditions ($\mathbf{u}^0_{hz}$). Panels (b-d): downwelling and upwelling areas associated with (b) losing, (c) neutral and (d) gaining conditions for one of the simulations reported by *Trauth et al.* [2013]. Blue and red regions indicate downwelling and upwelling, respectively; darker shading indicates where upwelling or downwelling has intensified while lighter shading indicate where upwelling or downwelling has weakened. The coordinate system indicates streambed elevation (z-axis), cross-stream direction (y-axis), and along-stream direction (x-axis). Note that only half of the stream width is pictured here. Elevation contours are shown in panels (b) through (d).

Accepted Article

This article is protected by copyright. All rights reserved.

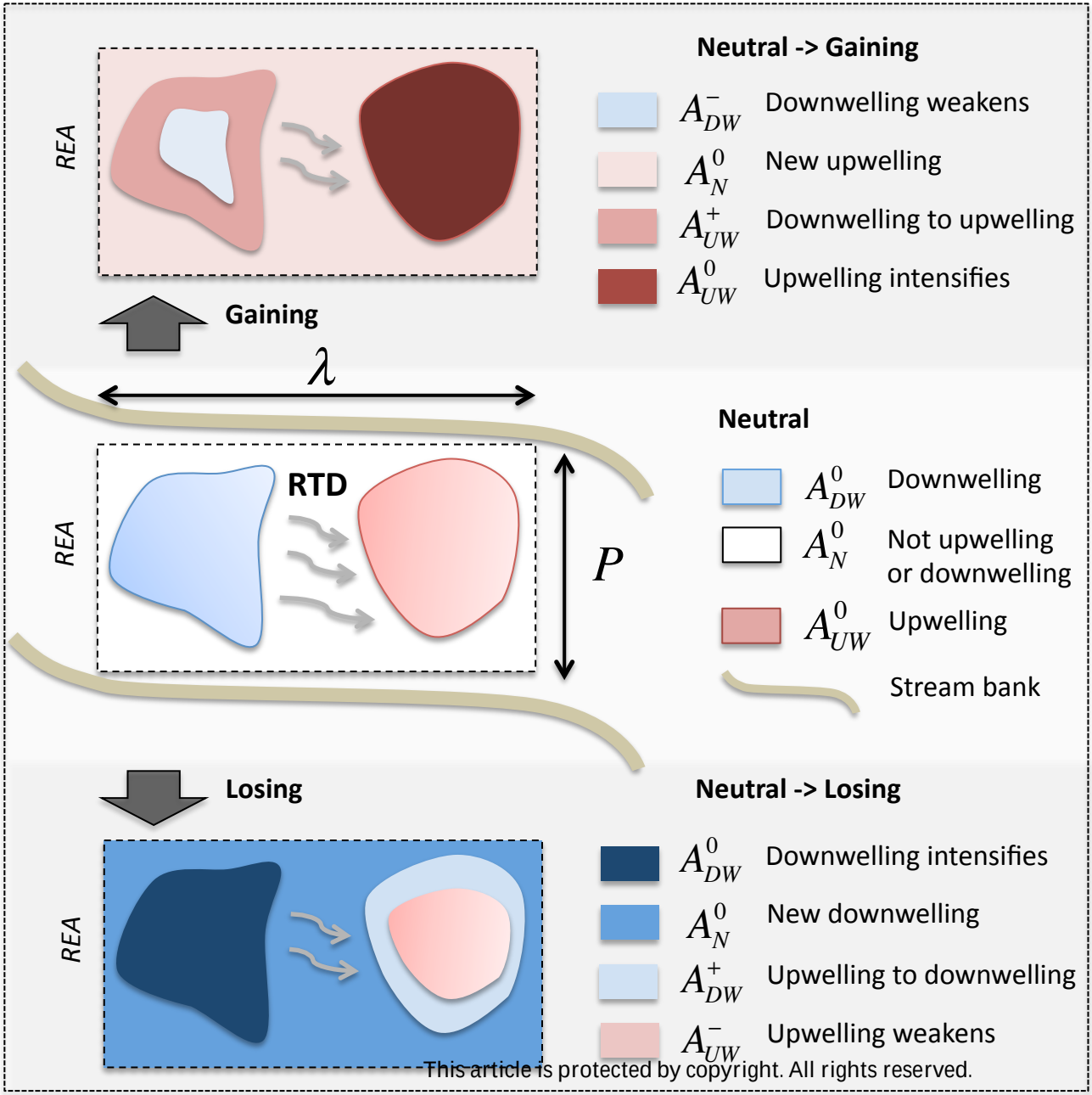

This article is protected by copyright. All rights reserved.

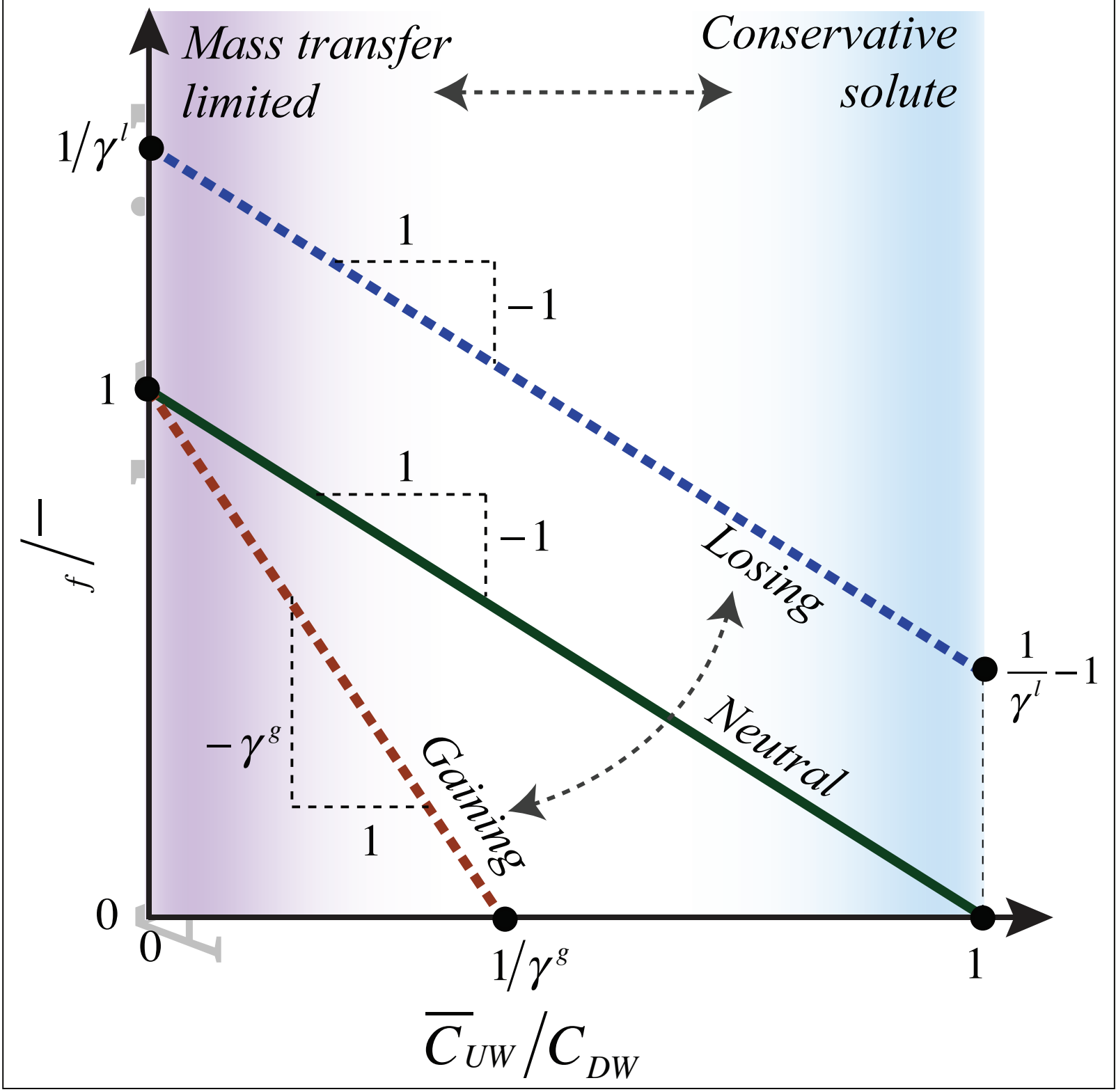

This article is protected by copyright. All rights reserved.

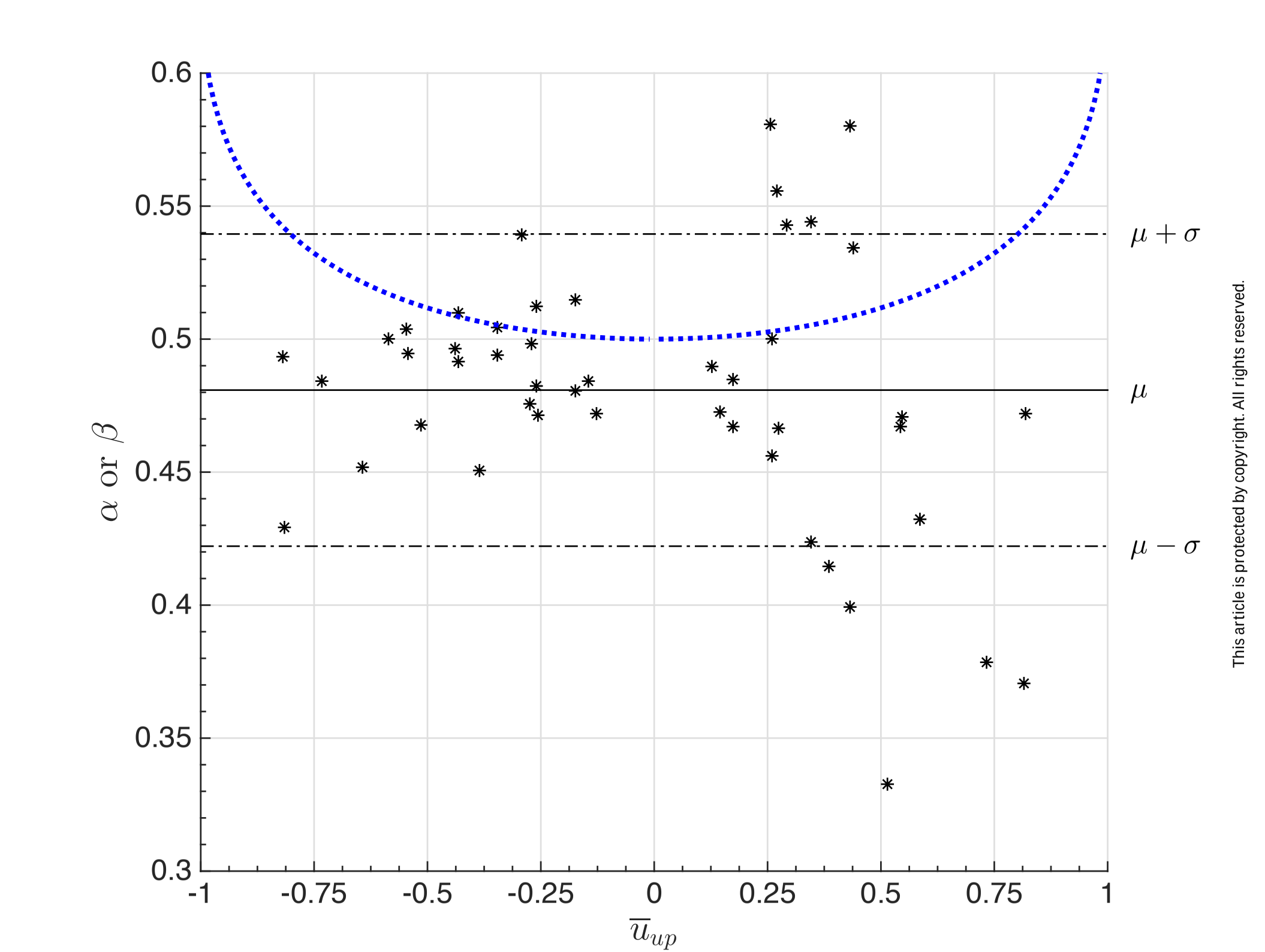

This article is protected by copyright. All rights reserved.

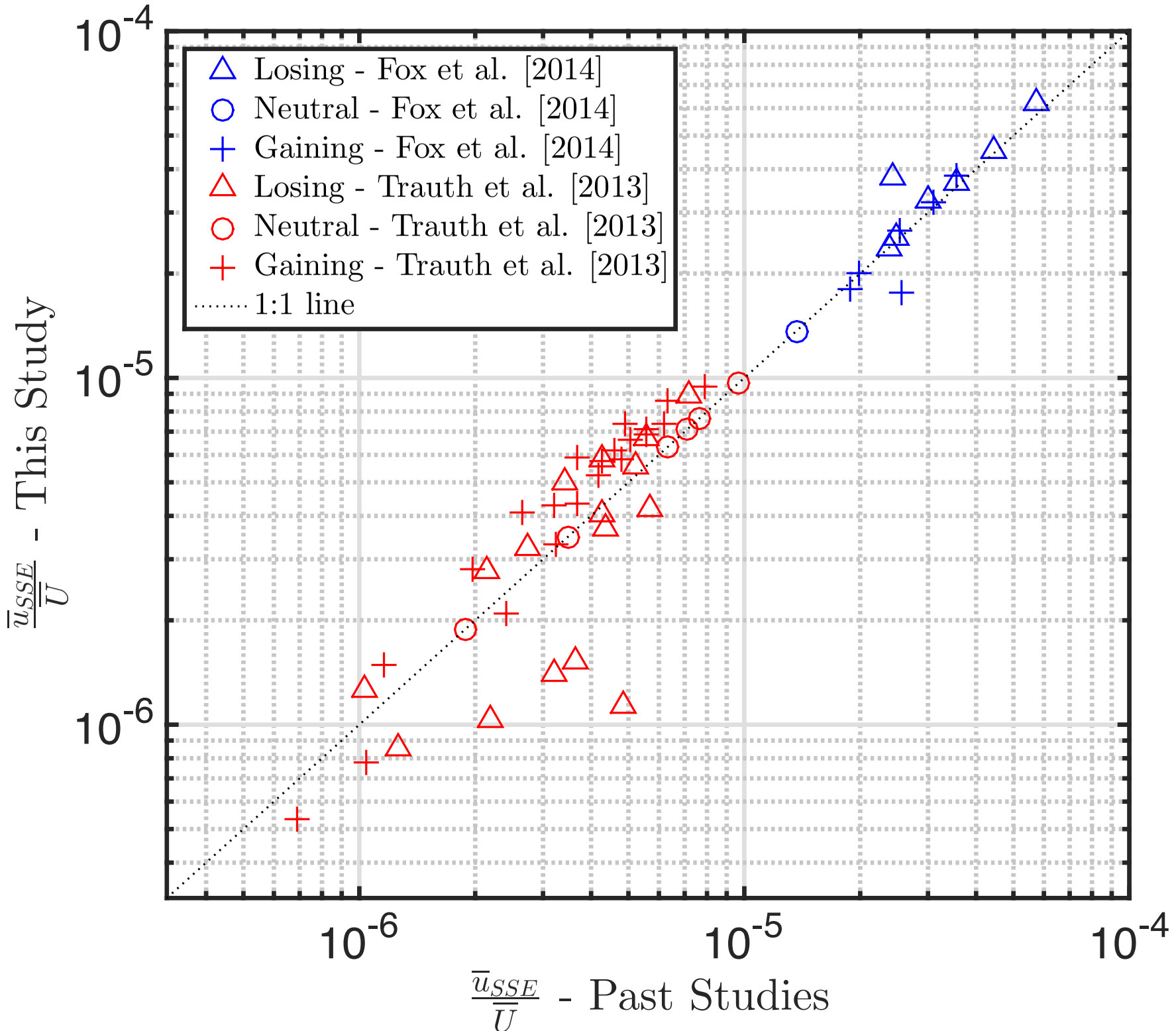

This article is protected by copyright. All rights reserved.

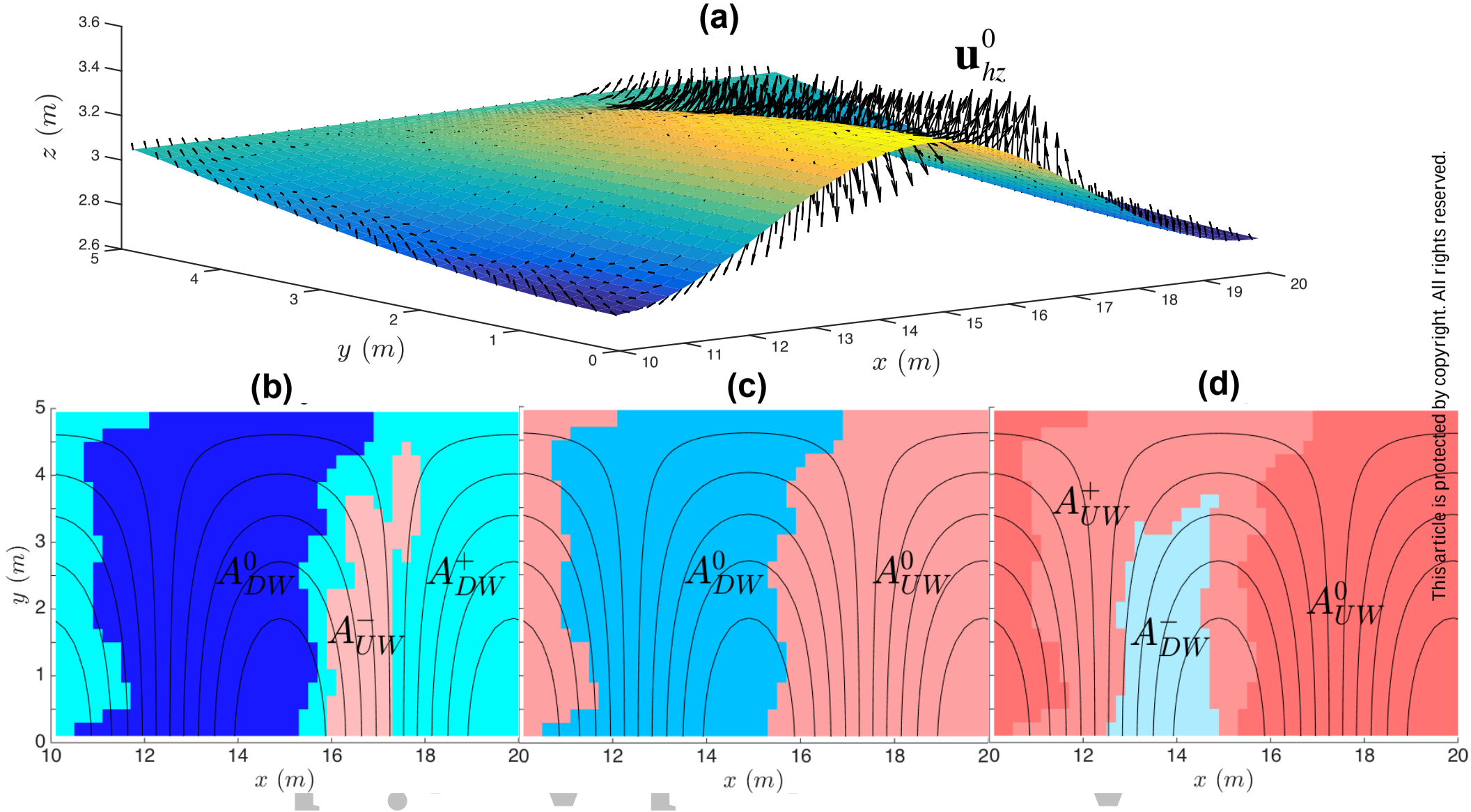

This article is protected by copyright. All rights reserved.